




Original Article

## Adsorption Ni(II) on Magnetic Fulvic Acid-Chitosan: Kinetics and Isotherm Study

Raihansyah Raja Utama<sup>1</sup>, Audrey Nur Aisyah<sup>1</sup>, Azzahra Sandri<sup>1</sup>, Mayang Fauziah Putri Kuntjahjono<sup>1</sup>, Sultan Napoleon<sup>1</sup>, Yusuf Bramastya Apriliyanto<sup>1</sup>, Nugroho Adi Sasongko<sup>2,3,4</sup>, Rahmat Basuki<sup>1\*</sup> 

<sup>1</sup>Department of Chemistry, The Republic of Indonesia Defense University, Kawasan IPSC Sentul, Bogor 16810, Indonesia

<sup>2</sup>Research Center For Sustainable Production System and Life Cycle Assessment, National Research and Innovation Agency (BRIN), KST Prof. BJ Habibie, Building 720 Puspiptek Area, South Tangerang, Banten 15314, Indonesia

<sup>3</sup>Energy Security Graduate Program, The Republic of Indonesia Defense University, Kawasan IPSC Sentul, Bogor 16810, Indonesia

<sup>4</sup>Murdoch University, 90 South St, Murdoch Western Australia 6150, Australia

<https://doi.org/10.55749/ss.v1i1.79>

Received: 27 May 2025; Revised: 4 Jun 2025; Accepted: 24 Jun 2025; Published online: 29 Jun 2025; Published regularly: 30 Jun 2025

This is an open access article under the CC BY-SA license (<https://creativecommons.org/licenses/by-sa/4.0/>).

**Abstract**— Indonesia, as one of the most populous countries in the world, requires clean water sources. Industrial waste that is improperly discharged pollutes water bodies with hazardous metals. Adsorption is one of the effective methods for reducing the concentration of harmful metals in water. This study utilized fulvic acid extracted from goat manure compost and combined it with chitosan and magnetite as an adsorbent material for Ni(II). The FTIR results for the magnetite-fulvic acid-chitosan composite showed a peak at 1627 cm<sup>-1</sup>, indicating the presence of aromatic C=C, aromatic ring -OH, and quinone C=O groups, which confirm the binding of fulvic acid. BET analysis was performed on magnetite and magnetite-fulvic acid-chitosan, and the pore volume and pore size were found to be 0.177488 cm<sup>3</sup>/g and 6.5394 nm, respectively. The composite exhibited magnetic behavior due to the attraction between the magnetite-fulvic acid-chitosan and an external magnet. Adsorption tests using isotherm and kinetic models revealed that Ni(II) adsorption followed a multilayer mechanism and pseudo-second-order kinetics, with a b value of 121.68 mg/g and an experimental q<sub>e</sub> of 6.28 × 10<sup>-5</sup> mol/g. This shows that the magnetite-fulvic acid-chitosan composite is a promising, sustainable, and magnetically separable adsorbent for the effective removal of nickel ions from contaminated water.

**Keywords**—Adsorption; Chitosan; Fulvic acid; Magnetite; Ni(II).

### 1. INTRODUCTION

Indonesia is the 4th most populous country after India, China, and the United States. As a country with the largest population, making the need for water for the people of Indonesia a basic necessity in everyday life [1]. Besides being needed by the human body, water also functions as a power plant in hydropower plants, washing, meeting agricultural and livestock needs, and others. Water is very easy to obtain because it can be found anywhere, such as rivers, lakes, dams, seas, raindrops, and waterways in the neighborhood. Indonesia as a tropical country has two seasons, namely the rainy season and the dry season [2]. With high rainfall in the rainy season, in some areas dams

are formed as water reservoirs. For example, the dam in Jatiluhur, West Java Province as the main source of water for the surrounding population.

The increasing construction of Industrial plants in Indonesia has led to concerns about water pollution due to the discharge of industrial waste into water bodies [8]. Several types of industries, such as textile, pharmaceutical, steel, and paper, are known to produce effluents containing harmful heavy metals, including Ni(II), Cd(II), Pb, Cr, Zn, and Fe. The presence of these metals in waters poses a threat to human health and ecosystems, as they are toxic and difficult to degrade naturally [3].

\*Corresponding author.

Email address: [rhmtbsq@gmail.com](mailto:rhmtbsq@gmail.com)

In waters, there are generally a lot of harmful heavy metals such as nickel(II). These metals are a serious threat because they are very difficult to decompose, so solutions are needed to remove or reduce the levels of these metals in water [4]. Various methods have been developed to reduce heavy metal contaminants in water, such as reverse osmosis, nanofiltration membranes, distillation, chemical precipitation, and filtration [5].

However, these methods often require high cost, high energy, specific operating conditions, or have low efficiency in treating dissolved metals. In contrast, adsorption methods are considered more economical, simple, and environmentally friendly, and allow the use of natural materials and organic waste as adsorbents [6]. In the last decade, the utilization of waste biomass as an adsorbent base material has continued to grow. Various organic wastes, such as sawdust waste [7], tea pulp waste [8], leather waste, and shell waste [9], have been shown to have potential as metal adsorbent materials due to their active functional group content and high cation exchange capacity (CEC). One compound that shows high ability in metal adsorption is humic acid because it is rich in negative ion charge, especially in the form of fulvic acid which is more soluble and active in aqueous conditions [10]. Humic acid sources generally come from peat soil, but the extraction process takes a long time, is not environmentally friendly, and contributes to carbon emissions. A more sustainable alternative is to utilize animal manure, such as cows, goats, and horses, which are known to contain humic and fulvic compounds [20]. Thus, it can reduce the use of peat soil that can damage the environment.

Nevertheless, the main drawback of humic acid is its low stability at acidic pH, so modification is needed to increase its effectiveness as an adsorbent. In some literature, it was found that there are modifying agents that are able to stabilize humic compounds in low pH, including bentonite [11], silica [12], double-layer hydroxy [13], chitin [14], and chitosan [15]. Chitosan is one of the modifying agents that can improve the stability and adsorption performance of humic compounds.

In addition, the addition of magnetic materials such as magnetite can facilitate the post-adsorption separation process. However, research on the utilization of humic acid from goat manure modified with chitosan and magnetite as a heavy metal adsorbent is still very limited. Therefore, this study aims to develop fulvic acid-based adsorbent material from goat manure modified with chitosan and magnetite ( $\text{Fe}_3\text{O}_4$ ) to increase the adsorption efficiency of Ni(II) metal ions. It is expected to contribute to heavy metal waste management efforts while supporting sustainable water security.

## 2. EXPERIMENTAL SECTION

### 2.1. Materials

The materials used in this study include fulvic acid derived from goat compost, as well as analytical-grade reagents produced by E. Merck for the extraction and

purification of fulvic acid, such as NaOH and HCl. The materials used for the synthesis of Fulvic Acid-Chitosan Magnetite include pure chitosan powder, alizarin red S solution, phenanthroline solution,  $\text{FeCl}_3 \cdot 6\text{H}_2\text{O}$ ,  $\text{FeSO}_4 \cdot 7\text{H}_2\text{O}$ , and  $\text{Ni}(\text{NO}_3)_2 \cdot 6\text{H}_2\text{O}$ . Other materials used include universal indicator, filter paper, and distilled water.

### 2.2. Instrumentation

The instruments used in this study include FTIR spectrometer (Prestige 21), Gas Sorption Analyzer (Micromeritics Tristar II 3020), and UV-Vis spectrophotometer (DLAB SP-UV1100).

### 2.3. Purification of Fulvic Acid from Goat Manure

Five hundred grams of finely ground goat manure compost were dissolved in 1 liter of 0.1 M NaOH solution and stirred at room temperature and pressure for 24 hours. The mixture was then separated by filtration, yielding a filtrate. This filtrate was acidified using 0.1 M HCl until the pH reached 1, resulting in the formation of two layers: the upper layer consisting of fulvic acid and the lower layer consisting of humic acid. The mixture was filtered again to separate the layers, and the resulting filtrate was then adjusted with NaOH until the pH reached 11.

### 2.4. Magnetite-AF-Chitosan Synthesis

The synthesis of fulvic acid–chitosan magnetite begins with the preparation of chitosan magnetite, followed by the immobilization of fulvic acid onto the chitosan magnetite. The synthesis of chitosan magnetite was carried out under a modified air atmosphere. A total of 0.1 g of chitosan was dispersed in 100 mL of 0.05 M acetic acid in a 250 mL Erlenmeyer flask. Then,  $\text{FeCl}_3 \cdot 6\text{H}_2\text{O}$  (4 g) and  $\text{FeSO}_4 \cdot 7\text{H}_2\text{O}$  (2 g) in a 2:1 molar ratio were added to the suspension. The resulting mixture was mechanically stirred for 3 minutes at room temperature.

Simultaneously, 25 mL of 25%  $\text{NH}_3$  and 50 mL of extracted fulvic acid were rapidly added to the mixture with vigorous stirring. The resulting black mixture was continuously stirred for 5 hours at  $75^\circ\text{C}$  under a closed air atmosphere. The mixture was then slowly cooled to room temperature over 24 hours. The resulting black precipitate was then separated from the solution and washed with distilled water.

### 2.5. Adsorption Isotherm

A total of 50 mg of fulvic acid–chitosan magnetite was interacted with 20 mL of metal ion solution with varying concentrations of 10, 20, 30, 50, 70, 100, and 200 mg/L for 2 hours. Each mixture was then filtered, and the filtrate was collected. The concentrations of metal ions before and after adsorption were complexed with phenanthroline for Ni(II) analysis, and then measured using a UV-Vis spectrophotometer.

## 2.6. Adsorption Kinetics

A total of 50 mg of fulvic acid–chitosan magnetite was interacted with 20 mL of 50 mg/L metal ion solution at the optimum pH. The mixture was then stirred for varying durations of 10, 20, 30, 40, 60, and 90 min. After reaching the specified time, each mixture was filtered, and the filtrate was collected. The concentration of adsorbate before and after adsorption was treated with phenanthroline for Ni(II) analysis and then measured using a UV-Vis spectrophotometer.

## 2.7. Preparation of Metal Standard Solution

Five 50 mL volumetric flasks were prepared with diluted metal ion solutions at concentrations of 10, 20, 30, 40, 50, 60, and 70 ppm. To each metal ion solution, one drop of phenanthroline solution was added, and the mixture was then shaken. The absorbance of each metal solution was measured using a UV-Vis spectrophotometer at wavelengths of 494.5 nm and 330 nm, and the absorbance values were recorded. The obtained absorbance values were plotted using Excel, and the resulting equation (Y) and correlation coefficient ( $R^2$ ) were noted.

## 3. RESULT AND DISCUSSION

### 3.1. Synthesis of Chitosan-AF Magnetite

The synthesis of fulvic acid–chitosan magnetite (AF-Chitosan) from goat manure compost was carried out using a one-pot method under basic conditions. This synthesis involved two main stages: the extraction of fulvic acid from goat manure compost and the one-pot synthesis process. The fulvic acid used was obtained from composted goat manure that had been dried over a long period. This is because uncomposted goat manure contains a high level of impurities, low concentrations of humic and fulvic acids, and a high moisture content [16]. The one-pot method used in this synthesis aimed to produce fulvic acid–chitosan magnetite by combining all the components (commercial chitosan, magnetite precursors, and fulvic acid extracted from goat manure) in a single vessel at once. Compared to other methods, such as the sol-gel method, which requires strict temperature and pH control, or the stepwise co-precipitation method, which involves gradual washing steps, the one-pot method offers a simpler and more environmentally friendly alternative for synthesizing adsorbent materials.

In the extraction of fulvic acid, dry goat manure compost was prepared and crushed in a mortar, then sieved using a 100 mesh sieve. According to Ayilara et al. (2014), this process aims to make the compost into a fine powder and increase the surface area, so that chemical reactions take place quickly and easily [17]. After being ground into a fine powder, the compost was dissolved in 1 L of 0.1 M NaOH for 24 hours. Following the addition of NaOH, the solution formed two phases, with the upper phase containing humic acid and fulvic acid. This is consistent with the Islam et al. (2020),

which states that at basic pH levels ( $>8$ ), both humic and fulvic acids are soluble [18]. The dissolved compounds were then separated and acidified with 0.1 M HCl until the pH reached 2. This process is known as deprotonation, in which the hydroxide ions ( $\text{OH}^-$ ) in the basic solution attract protons from the carboxylic acid groups ( $-\text{COOH}$ ), forming carboxylate ions ( $-\text{COO}^-$ ) and water ( $\text{H}_2\text{O}$ ). As a result, humic substances become soluble, while humin remains insoluble.

The one-pot method begins with solid chitosan being dissolved in 0.05 M acetic acid for 1 hour in an Erlenmeyer flask, as shown in **Figure 1**. Acidic solutions such as acetic acid are effective solvents for chitosan. As explained by Giraldo and Rivas (2021), acetic acid promotes greater dissociation or increases the level of ionization, resulting in a higher concentration of amine groups ( $\text{NH}_3^+$ ) [19], as illustrated in **Figure 2(a)**.

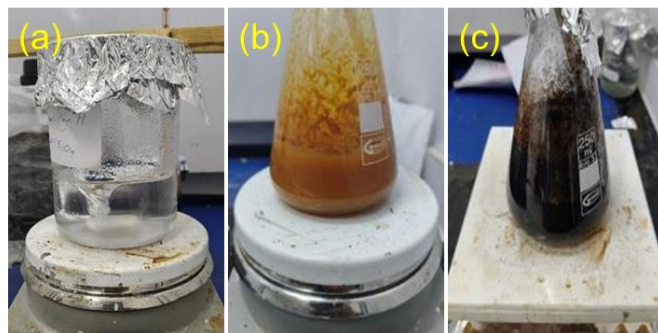


**Figure 1.** Chitosan is dissolved in acetic acid (a),  $\text{Fe}^{2+}$  and  $\text{Fe}^{3+}$  ions are mixed into the chitosan solution (b), and fulvic acid and  $\text{NH}_4\text{OH}$  are mixed (c)

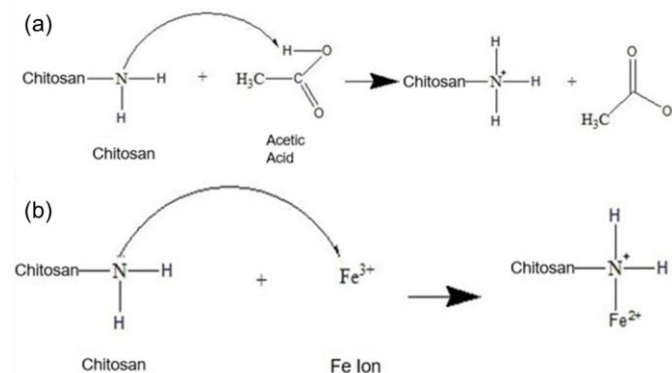


**Figure 2.** (a) Reaction of chitosan with acetic acid (b) Chemical reaction of chitosan with  $\text{Fe}^{3+}$  ions

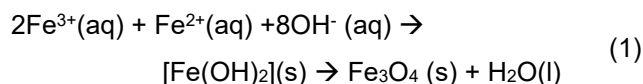
When the amine groups on chitosan increase, the chitosan polymer chains experience strong repulsion, resulting in larger pore volumes that can bind other compounds. The process continues by simultaneously adding  $\text{FeCl}_3 \cdot 6\text{H}_2\text{O}$  and  $\text{FeSO}_4 \cdot 7\text{H}_2\text{O}$ , in a 2:1 molar ratio, as magnetite precursors. This mixture is then heated at  $80^\circ\text{C}$  for 4 h.

As explained in the literature by Parajuli et al. (2020), the synthesized magnetite has a  $\text{Fe}^{3+}$  to  $\text{Fe}^{2+}$  ratio of 2:1 (mol/mol). This 2:1 molar ratio is essential to obtain pure magnetite; if the molar ratio deviates, other iron oxide compounds may form instead of magnetite. The combination of  $\text{Fe}^{3+}$  and  $\text{Fe}^{2+}$  ions, as illustrated in



**Figure 1**, takes place over 4 hours at 80°C in a closed system. This condition is intended to accelerate the reduction of  $\text{Fe}^{2+}$  and  $\text{Fe}^{3+}$  and to allow uniform ion diffusion, thereby minimizing the possibility of  $\text{Fe}^{2+}$  and  $\text{Fe}^{3+}$  oxidation, which could lead to the formation of  $\text{Fe}_2\text{O}_3$  or  $\text{FeO}(\text{OH})$  [20].

Then, the extracted fulvic acid and concentrated  $\text{NH}_4\text{OH}$  were added simultaneously and rapidly to the mixture. Upon the addition of concentrated  $\text{NH}_4\text{OH}$ , the mixture precipitates and changes color to black. The total chemical reaction is:



The precipitate formed in the mixture is due to the change from an acidic to a basic environment. This precipitation process is known as co-precipitation. According to Ismail et al. (2024),  $\text{NH}_4\text{OH}$  acts as a precipitating agent in this method and results in homogeneous magnetite with higher crystallinity compared to using strong bases such as  $\text{NaOH}$  [21]. Another function of chitosan is to act as a binder or linker between the magnetite and the fulvic acid, which is in the liquid phase, thereby forming a homogeneous solid that is insoluble at neutral pH.

The mixture was then left to stand for 24 hours and washed until the pH reached 7. Afterward, the sample was placed in an oven for drying and subsequently subjected to characterization and adsorption tests. The reaction scheme for the formation of fulvic acid–chitosan magnetite is illustrated in the diagram shown in **Figure 3**.

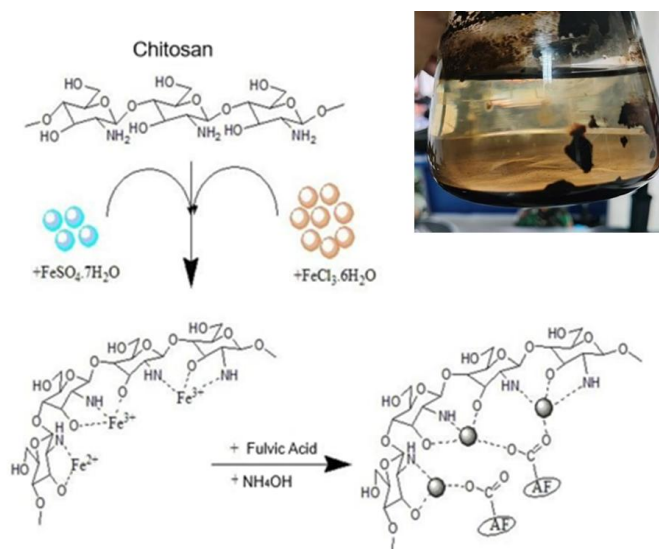


**Figure 3.** Schematic representation of Fulvic Acid-Magnetite-Chitosan synthesis

### 3.2. Characterization of Fulvic Acid-Magnetite-Chitosan

Based on the FTIR test data, the samples can be identified by their functional groups. FTIR characterization was carried out in the wavelength range of 500 nm to 4000 nm. The samples tested on

FTIR were commercial chitosan, extracted fulvic acid, magnetite, and chitosan-fulvic acid magnetite. The results obtained in the form of FTIR spectra and absorption peak tables as shown in **Figure 4** and **Table 1**.

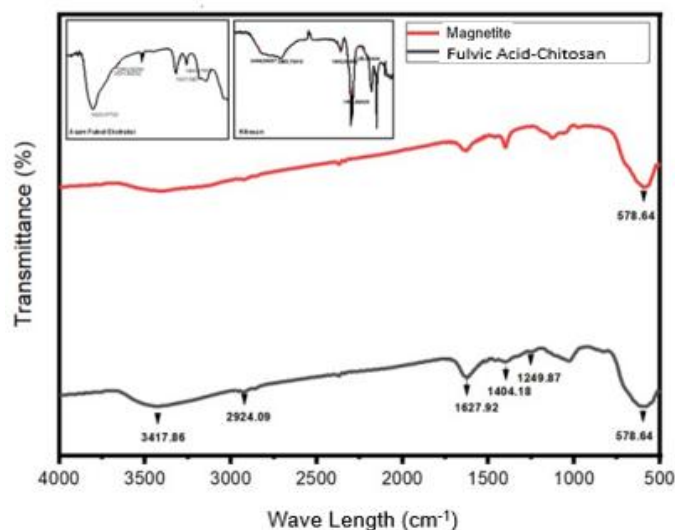


**Figure 4.** FTIR characterization results of extracted fulvic acid, chitosan, magnetite, and fulvic acid-chitosan magnetite

In the chitosan test results, the M absorption region appears at  $3448\text{ cm}^{-1}$  which indicates the stretching absorption of the NH and OH combination. While in the  $1653\text{ cm}^{-1}$  region, it indicates the bending vibrations of NH and C=O [22]. Then at wave number  $1180\text{ cm}^{-1}$  indicates the vibrations of C-O and CN. The successful extraction of fulvic acid from goat manure can be seen in the absorption area of 5 peaks as in research [23], namely at  $3425\text{ cm}^{-1}$  (OH and NH groups),  $2931\text{ cm}^{-1}$  (C-H aliphatic),  $1627\text{ cm}^{-1}$  (COO-anti-symmetric and NH amine)  $1404\text{ cm}^{-1}$  (CO and OH carboxyl), and  $1103\text{ cm}^{-1}$  (C-O aliphatic ether). In the absorption band belonging to  $\text{Fe}_3\text{O}_4$ , the peak appears at  $578\text{ cm}^{-1}$  which is the Fe-O stretching vibration so that its existence has proven the formation of  $\text{Fe}_3\text{O}_4$  [24].

The magnetite-chitosan-AF sample was initiated by the immobilization of fulvic acid on magnetite-chitosan. Magnetite-chitosan was synthesized through a coprecipitation process using  $\text{NH}_4\text{OH}$  solvent in an alkaline atmosphere. In **Figure 8**, the results of FTIR characterization of magnetic fulvic acid-chitosan, the presence of  $\text{Fe}_3\text{O}_4$  is evident with the absorption peak at  $578\text{ cm}^{-1}$ , where Fe-O stretching vibrations occur [30]. After the formation of the mixed composite, the O-H and N-H vibrations at  $3425\text{ cm}^{-1}$  (belonging to fulvic acid) shifted to  $3417\text{ cm}^{-1}$  after becoming fulvic acid-chitosan magnetite. This is due to the interaction of FeO with -OH bonds and -NH stretching vibrations in chitosan [3]. Then in the  $1627\text{ cm}^{-1}$  absorption region, it shows the presence of C=C aromatic and aromatic rings formed by OH bonds and C=O quinone groups, which are characteristics of fulvic acid bound to the composite. At peak  $1249\text{ cm}^{-1}$ , indicating the composite formed chitosan originally from  $1234\text{ cm}^{-1}$ . This shift is caused

**Table 1.** FTIR absorption peak of Fe<sub>3</sub>O<sub>4</sub>-Chitosan-FA

Fulvic Acid (FA)	Absorption peak (cm <sup>-1</sup> )			Vibrational group
	Chitosan	Fe <sub>3</sub> O <sub>4</sub>	Fe <sub>3</sub> O <sub>4</sub> -Chitosan-FA	
3425	3448	3402	3417	(-OH) stretching
2931, 2862	2869	2924, 2862	2924, 2855	(-CH) aliphatic stretching
1627	1662	-	1627	(-NH) bending
1572	1554	-	1519	(-NO) stretching
1404	1417	-	1404	(-COO <sup>-</sup> ) stretching
1103	1180	-	1156	(-CO) eter stretching & (CN) stretching
-	1234	-	1249	(-CN) bending
-	-	578	578	(-FeO) stretching

by the interaction or formation of new bonds between chitosan and other materials, so that the (-CN) group becomes stiffer or stronger.

The synthesized chitosan-AF magnetite and magnetite were characterized using Brunauer-Emmett-Teller (BET) and the results are shown in **Figure 5**. The results of N<sub>2</sub> adsorption-desorption isotherms on magnetite chitosan-AF and magnetite adsorbents are represented as in **Table 2**. The increase in pore volume and diameter as well as the decrease in specific surface area value of magnetite chitosan-AF than magnetite are caused by chitosan binding to magnetite. Chitosan that binds to magnetite allows aggregation and forms aggregates [25], thus clogging small pores and creating new larger pores. Chitosan and fulvic acid, which are organic compounds, when aggregated and form a new layer on the magnetite surface, some active sites are covered and the active surface area is reduced. However, due to its loose and flexible structure, chitosan can also create additional large voids or pores.

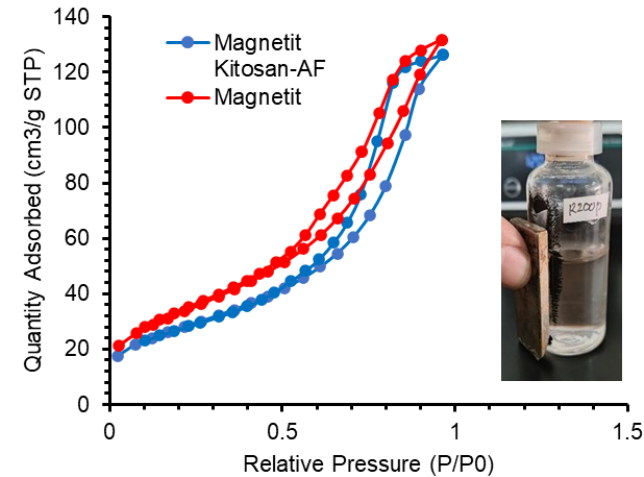


**Figure 5.** BET analysis results of magnetite-chitosan-FA and magnetite

In **Figure 5**, the graph formed corresponds to the characteristics of type IV(a) isotherms based on IUPAC categories, where adsorption is influenced by adsorbent and adsorbate interactions as well as interactions within molecules in a condensed state on mesoporous adsorbents [26]. The pore diameter size obtained in **Table 2** has a value of more than 5, this is consistent with the research of Kyriakopoulos et al. (2024) where

type IV with a pore size of 2-50 nm experiences capillary condensation [26]. Capillary condensation is the cause of the formation of loop hysteresis at relative pressures between 0.55-0.8.

**Table 2.** Adsorbent parameters of N<sub>2</sub> adsorption isotherm calculation results

Adsorbent	S <sub>BET</sub> (m <sup>2</sup> g <sup>-1</sup> )	V <sub>total</sub> (cm <sup>3</sup> g <sup>-1</sup> )	Pore size (nm)
Magnetite	52.095	0.169	5.610
Magnetite Chitosan- AF	46.018	0.177	6.539

Based on the FTIR test results of AF-chitosan magnetite, it was detected that the composite has Fe-O vibrations which indicate the presence of magnetite formed. However, the presence of magnetite, besides being verified by IR spectrum, can be verified by other methods. One of the properties possessed by magnetite is strong magnetic properties, called supermagnetic. Qualitatively, the magnetic properties can be analyzed simply by bringing the AF-chitosan magnetite closer to an external magnetic bar. If the composite has magnetic properties. it will tend towards the direction of the external magnetic bar. The test was conducted as shown in **Figure 5**. As shown, the AF-chitosan magnetite composite exhibited magnetic attraction when placed near an external magnet. This confirms that the synthesized AF-chitosan magnetite possesses magnetic properties. These magnetic properties will be utilized in the adsorption experiments. In this study. the separation method for the adsorption products will use an external magnet instead of filtration with filter paper. This approach offers a simpler. faster. and more practical method.

**3.3. Ni(II) Standard Solution**

The prepared metal ion solution was added with the metal-complexing agent, phenanthroline. Then, the metal solution was analyzed using a UV-Vis spectrophotometer. The standard metal solutions tested at a wavelength range of 330 nm. The absorbance data of standard Ni metal solutions complexed with phenanthroline at concentrations of 0, 10, 20, 30, 40, 50, 60, and 70 mg/L were plotted with absorbance values on the Y-axis and concentration values on the X-axis, as shown in Figure 12. The plotted data produced a linear equation of  $y = 0.012x + 0.0015$  with a correlation



coefficient ( $R^2$ ) of 0.9995. The sensitivity of the Ni-phenanthroline standard series method was 0.012, meaning that for every 1 ppm increase in  $Ni^{2+}$  concentration, the signal increases by 0.012 absorbance units. Therefore, the sensitivity of this standard series is considered relatively high. The correlation coefficient value being very close to 1 indicates that the method is highly accurate.

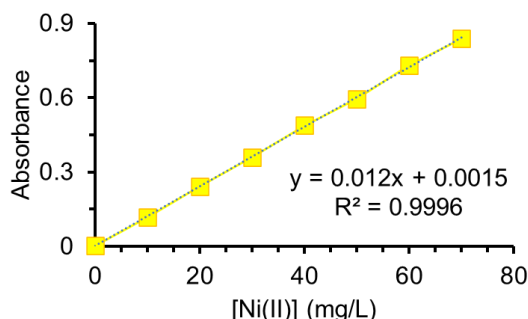


**Figure 6.** Standard calibration curve graph of nickel-phenanthroline metal series

### 3.4. Isotherm Study

The Ni metal solutions adsorbed by fulvic acid-chitosan magnetite at various concentrations were filtered, and the resulting filtrates were tested using a UV-Vis spectrophotometer after being treated with the complexing agent phenanthroline. The obtained data were then processed to be applied to the Langmuir, Freundlich, Dubinin-Radushkevich, and Temkin isotherm equations. After processing the data, the values were plotted on the x and y axes to create graphs, as shown in **Figure 7**.

Based on the data plotted using the Langmuir, Freundlich, Dubinin-Radushkevich (DR), and Temkin isotherm models, the equations and correlation coefficients ( $R^2$ ) for each graph were obtained. For the Langmuir and Freundlich models, the Freundlich model showed a higher  $R^2$  value of 0.9998 compared to Langmuir's 0.9851. This indicates that the adsorption of Ni(II) ions on fulvic acid-chitosan magnetite occurs via multilayer or heterogeneous adsorption. The high adsorption capacity of 121.68 mg/g obtained for the magnetite-fulvic acid-chitosan composite in this study significantly exceeds that reported for pure chitosan-magnetite (30.03 mg/g) [27].

This increase is due to the synergistic effect of fulvic acid and chitosan, which provides more active sites and enhances the interaction with Ni(II) ions. Multilayer or multi-energy adsorption suggests the formation of two layers of  $Ni^{2+}$  ions on the adsorbent surface, involving functional groups such as (-COOH) from fulvic acid, (-OH) from magnetite and chitosan, and (-NH<sub>2</sub>) from chitosan. Furthermore, from the Freundlich model's equation, the multilayer adsorption capacity (B) was found to be 6826.44 mg/g, which represents the relative adsorption capacity of the adsorbent for multilayer adsorption on the surface. Meanwhile, the Langmuir model yielded a monolayer adsorption capacity (b) of

121.68 mg/g and an adsorption energy ( $E_L$ ) of 11.49 kJ/mol. The Langmuir constant  $K_L$  of 103.57 L/mol indicates a very strong interaction and high affinity between the fulvic acid-chitosan magnetite and  $Ni^{2+}$  ions. However, the value of B suggests a lower adsorption capacity, meaning that the Langmuir isotherm model tends to emphasize the binding strength ( $K_L$ ) more than the adsorption capacity (b).

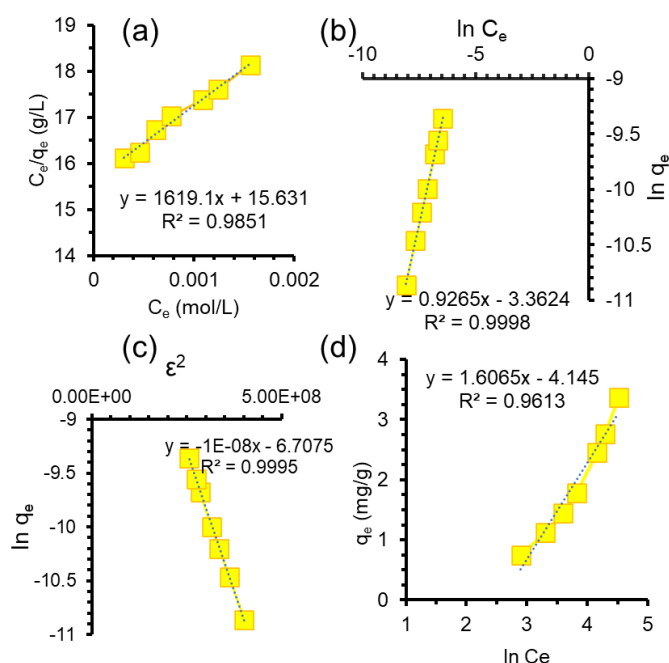


**Figure 7.** Plot of linear Langmuir (a), Freundlich (b), Temkin (c), and Dubinin-Radushkevich (d) isotherm adsorption model graphs of Ni(II) onto Magnetite-chitosan-AF

In the Dubinin-Radushkevich (DR) plot, the linear equation obtained was  $y = 1.6065x - 4.145$  with a coefficient of determination  $R^2 = 0.9613$ . Based on this linear regression, the DR model parameters were determined as follows: the adsorption capacity QDR was 240.7 mg/g, the constant  $B_{DR}$  was  $2.08 \times 10^{-7}$  mol<sup>2</sup>/J<sup>2</sup>, and the mean adsorption energy  $E_{DR}$  was 6.936 kJ/mol. The  $E_{DR}$  value derived from the DR isotherm can be used to predict the adsorption energy at the sixth layer of Ni(II), in comparison with the adsorption energy at the first layer of Ni(II) obtained from the Langmuir model. A clear decrease in adsorption energy is observed from the first layer of Ni(II) ( $E_L = 11.49$  kJ/mol) to the sixth layer of Ni(II) ( $E_{DR} = 6.93$  kJ/mol). The  $E_{DR}$  value below 8 kJ/mol indicates that the adsorption mechanism is predominantly physical in nature.

This physisorption process is attributed to Van der Waals interactions and hydrogen bonding involving active functional groups such as (-NH<sub>2</sub>), (-OH), and (-COOH). For the Temkin isotherm model, the linearized form yielded the equation  $y = -1.039E-08x - 6.7074$  with an excellent fit, indicated by  $R^2 = 0.9995$ . The Temkin constant ( $b_T$ ) was determined to be 1542.21 J/mol, which represents the binding energy between adsorbate and adsorbent per mole. Accordingly,  $b_T$  can be



interpreted as the adsorption energy of the outermost Ni(II) layer on the fulvic acid-chitosan magnetite composite.

### 3.5. Kinetics Study

The Ni metal solution adsorbed by fulvic acid-chitosan magnetite at various shaker times was filtered, and the resulting filtrate was analyzed using UV-Vis spectrophotometry after the addition of the complexing agent, phenanthroline. The obtained data were processed to be applied in the Lagergren and Ho kinetic equations. After processing, the data were plotted on the x and y axes to construct the corresponding graphs, as shown in **Figure 8**.

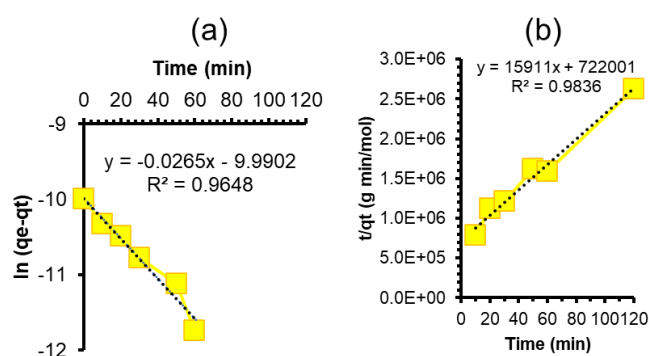


**Figure 8.** Plot of Lagergren (a) and Ho (b) kinetic adsorption model graphs of Ni(II) onto Magnetite-chitosan-FA

Based on the data plotted using the Lagergren and Ho kinetic models as a function of time, the amount of Ni metal adsorbed at equilibrium, denoted as the experimental  $q_e$  was recorded as  $4.57 \times 10^{-5}$  mol/g of adsorbent. The Ho kinetic model best represents the adsorption of Ni metal, as indicated by the highest correlation coefficient  $R^2 = 0.9836$ . This suggests that the Ni adsorption process predominantly follows the Ho kinetic model, implying that chemisorption is the dominant adsorption mechanism. From the Ho kinetic model equation, the adsorption rate constant ( $k_{Ho}$ ) was determined to be 350.63 g/mol·min, and the equilibrium adsorption capacity was calculated as  $6.28 \times 10^{-5}$  mol/g. However, the Ho kinetic model cannot be directly cross-validated with adsorption isotherm parameters. To enable comparison with isotherm parameters, the adsorption equilibrium constant  $K$  can be derived from the relation  $K = k_{ads}/k_{des}$ , where  $K$  serves as the adsorption parameter allowing cross-study. In the Ho kinetic model, the calculated  $q_e$  ( $4.57 \times 10^{-5}$  mol/g) closely matches the experimental  $q_e$  ( $6.28 \times 10^{-5}$  mol/g), confirming that the adsorption process adheres well to the Ho kinetic model.

### 4. CONCLUSION

Fulvic acid was obtained by extraction from goat manure compost using an acid-base precipitation method. The extracted fulvic acid was then combined with chitosan and magnetite ( $Fe^{3+}/Fe^{2+}$ , molar ratio 2:1) via a one-pot synthesis method, yielding a fulvic acid-

chitosan magnetite composite. The composite was characterized by FTIR, showing absorption peaks similar to those of chitosan, magnetite, and fulvic acid. Both magnetite and the composite were further characterized by BET analysis to determine specific surface area, pore volume, and pore size. The results indicated a pore volume of  $0.177488 \text{ cm}^3/\text{g}$ , an average pore diameter of  $6.5394 \text{ nm}$ , and a specific surface area of  $46.0188 \text{ m}^2/\text{g}$ . Magnetic property testing of the composite using an external magnet demonstrated magnetic attraction between the external magnet and the composite.

The adsorption of Ni-phenanthroline complexes was found to proceed via multilayer adsorption, as evidenced by the Freundlich isotherm with a high correlation coefficient  $R^2=0.999$ , an adsorption capacity of  $6826.44 \text{ mg/g}$ , and an intensity parameter of 1.07. According to the Langmuir model, the adsorption capacity (b) was  $121.68 \text{ mg/g}$ , the adsorption energy  $E_L$  was  $11.49 \text{ kJ/mol}$ , and the Langmuir constant  $K_L$  was  $103.57 \text{ L/mol}$ . The Dubinin-Radushkevich ( $D_R$ ) model yielded a mean adsorption energy  $E_{DR}$  of  $6.936 \text{ kJ/mol}$ , whereas the Temkin model produced an energy constant ( $b_T$ ) of  $1542.21 \text{ J/mol}$ . Furthermore, the kinetics of Ni adsorption followed a pseudo-second-order model (Ho) with a correlation coefficient  $R^2 = 0.9836$ . The Ho model provided calculated and experimental equilibrium adsorption capacities ( $q_e$ ) of  $4.57 \times 10^{-5} \text{ mol/g}$  and  $6.28 \times 10^{-5} \text{ mol/g}$ , respectively.

### SUPPROTING INFORMATION

There is no supporting information in this paper. The data supporting this research's findings are available on request from the corresponding author (R.Basuki).

### ACKNOWLEDGEMENT

The authors sincerely acknowledge the financial support provided by the Department of Chemistry, Republic of Indonesia Defense University. The authors also extend their gratitude for the facilities and laboratory resources made available by the BRIN.

### CONFLICT OF INTEREST

There was no conflict of interest in this study.

### AUTHOR CONTRIBUTIONS

RB, YBA, and NAS performed the conceptualization, investigation, supervision, writing original draft, review & editing. RRH, MFPK, and SN conducted the experiment, wrote and revised the manuscript. All authors approved the final version of the manuscript.

### REFERENCES

- [1] Mutoffar, M.M., Naseer, M. and Fadillah, A. 2022. Klasifikasi kualitas air sumur menggunakan algoritma random forest. *Naratif: Jurnal Nasional Riset, Aplikasi dan Teknik Informatika*. 4(2). 138-146. Doi: <https://doi.org/10.53580/naratif.v4i2.160>.
- [2] Dewi, E.P., Wijaya, A., Sujatini, S., Rahmana, D., Mandela, C.

- and Gulit, F. 2020. Penerapan Double Skin Facade Pada Daerah Iklim Tropis. *IKRA-ITH Teknologi Jurnal Sains dan Teknologi*. 4(2).1-7.
- [3] Tran, H.V., Dai Tran, L. and Nguyen, T.N. 2010. Preparation of chitosan/magnetite composite beads and their application for removal of Pb(II) and Ni(II) from aqueous solution. *Mater. Sci. Eng., C*. 30(2). 304-310. Doi: <https://doi.org/10.1016/j.msec.2009.11.008>.
- [4] Anderson, A., Anbarasu, A., Pasupuleti, R.R., Manigandan, S., Praveenkumar, T.R. and Kumar, J.A. 2022. Treatment of heavy metals containing wastewater using biodegradable adsorbents: A review of mechanism and future trends. *Chemosphere*. 295. 133724. Doi: <https://doi.org/10.1016/j.chemosphere.2022.133724>.
- [5] Carmona, B. and Abejón, R. 2023. Innovative membrane technologies for the treatment of wastewater polluted with heavy metals: perspective of the potential of electrodialysis, membrane distillation, and forward osmosis from a bibliometric analysis. *Membranes*. 13(4). 385. Doi: <https://doi.org/10.3390/membranes13040385>.
- [6] Rashid, R., Shafiq, I., Akhter, P., Iqbal, M.J. and Hussain, M. 2021. A state-of-the-art review on wastewater treatment techniques: the effectiveness of adsorption method. *Environ. Sci. Pollut. Res.* 28. 9050-9066. Doi: <https://doi.org/10.1007/s11356-021-12395-x>.
- [7] Chikri, R., Elhadiri, N., Benchanaa, M. and El Maguana, Y. 2020. Efficiency of sawdust as low - cost adsorbent for dyes removal. *J. Chem.* 2020(1). 8813420. Doi: <https://doi.org/10.1155/2020/8813420>.
- [8] Ateş, A., Mert, Y. and Timko, M.T. 2023. Evaluation of characteristics of raw tea waste-derived adsorbents for removal of metals from aqueous medium. *Biomass Convers. Biorefin.* 13. 7811-7826. Doi: <https://doi.org/10.1007/s13399-021-01721-5>.
- [9] Tamjidi, S. and Ameri, A. 2020. A review of the application of sea material shells as low cost and effective bio-adsorbent for removal of heavy metals from wastewater. *Environ. Sci. Pollut. Res.* 27(25). 31105-31119. Doi: <https://doi.org/10.1007/s11356-020-09655-7>.
- [10] Boguta, P. and Sokółowska, Z. 2020. Zinc binding to fulvic acids: Assessing the impact of pH, metal concentrations and chemical properties of fulvic acids on the mechanism and stability of formed soluble complexes. *Molecules*. 25(6). 1297. Doi: <https://doi.org/10.3390/molecules25061297>.
- [11] Ewis, D., Mahmud, N., Benamor, A., Ba-Abbad, M.M., Nasser, M. and El-Naas, M. 2022. Enhanced removal of diesel oil using new magnetic bentonite-based adsorbents combined with different carbon sources. *Water, Air, & Soil Pollution*. 233(6). 195. Doi: <https://doi.org/10.1007/s11270-022-05641-6>.
- [12] Ngatiyo, Basuki, R., Rusdianso, B., Nuryono. 2020. Sorption-desorption profile of Au(III) onto silica modified quaternary amines (SMQA) in gold mining effluent. *J. Environ. Chem. Eng.* 8(3). 103747. Doi: <https://doi.org/10.1016/j.jece.2020.103747>.
- [13] Yadav, B.S. and Dasgupta, S. 2022. Effect of time, pH, and temperature on kinetics for adsorption of methyl orange dye into the modified nitrate intercalated MgAl LDH adsorbent. Yadav, B.S. and Dasgupta, S., 2022. Effect of time, pH, and temperature on kinetics for adsorption of methyl orange dye into the modified nitrate intercalated MgAl LDH adsorbent. *norg. Chem. Commun.* 137. 109203. Doi: <https://doi.org/10.1016/j.inoche.2022.109203>.
- [14] Basuki, R., Apriliyanto, Y.B., Stiawan, E., Pradipta, A.R., Rusdianso, B. and Putra, B.R., 2025. Magnetic hybrid chitin-horse manure humic acid for optimized Cd(II) and Pb(II) adsorption from aquatic environment. *Case Stud. Chem. Environ. Eng.* 101138. Doi: <https://doi.org/10.1016/j.csee.2025.101138>.
- [15] da Silva Alves, D.C., Healy, B., Pinto, L.A.D.A., Cadaval Jr, T.R.S.A. and Breslin, C.B. 2021. Recent developments in chitosan-based adsorbents for the removal of pollutants from aqueous environments. *Molecules*. 26(3). 594. Doi: <https://doi.org/10.3390/molecules26030594>.
- [16] Rana, T. and Roy, A. 2024. Goat manure production and waste management. *Trends in Clinical Diseases, Production and Management of Goats*. 203-215. Doi: <https://doi.org/10.1016/B978-0-443-23696-9.00007-9>.
- [17] Ayilara, M.S., Olanrewaju, O.S., Babalola, O.O. and Odeyemi, O. 2020. Waste management through composting: Challenges and potentials. *Sustainability*. 12(11). 4456. Doi: <https://doi.org/10.3390/su12114456>.
- [18] Islam, M.A., Morton, D.W., Johnson, B.B. and Angove, M.J. 2020. Adsorption of humic and fulvic acids onto a range of adsorbents in aqueous systems, and their effect on the adsorption of other species: A review. *Sep. Purif. Technol.* 247. 116949. Doi: <https://doi.org/10.1016/j.seppur.2020.116949>.
- [19] Giraldo, J.D. and Rivas, B.L. 2021. Direct ionization and solubility of chitosan in aqueous solutions with acetic acid. *Polymer Bulletin*. 78. 1465-1488. Doi: <https://doi.org/10.1007/s00289-020-03172-w>.
- [20] Blowes, D., Ptacek, C., Jambor, J. and Weisener, C. 2005. The geochemistry of acid mine. *Environ. Geochem.* 9. 149.
- [21] Ismail, H., Zainuddin, Z., Mohamad, H. and Hamid, M.A.A., 2022. Compatibility of Concentrated NaOH as a Precipitation Agent in the Synthesis of Maghemite ( $\gamma\text{-Fe}_2\text{O}_3$ ) Nanoparticles via Co-precipitation Method. *J. Phys. Sci.* 33(2). 61-75. Doi: <https://doi.org/10.21315/jps2022.33.2.4>.
- [22] Zhuang, J., Li, M., Pu, Y., Ragauskas, A.J. and Yoo, C.G. 2020. Observation of potential contaminants in processed biomass using fourier transform infrared spectroscopy. *Appl. Sci.* 10(12). 4345. Doi: <https://doi.org/10.3390/app10124345>.
- [23] Gong, G., Xu, L., Zhang, Y., Liu, W., Wang, M., Zhao, Y., Yuan, X. and Li, Y., 2020. Extraction of fulvic acid from lignite and characterization of its functional groups. *ACS Omega*. 5(43). 27953-27961. Doi: <https://doi.org/10.1021/acsomega.0c03388>.
- [24] Reyes, M., Herrera, G., Escudero, R., Patiño, F., Reyes, I.A., Flores, M., Palacios, E.G., Juárez, J. and Barrientos, F. 2022. Surface spectroscopy of pyrite obtained during grinding and its magnetisation. *Minerals*. 12(11). 1444. Doi: <https://doi.org/10.3390/min12111444>.
- [25] Brião, G.D.V., De Andrade, J.R., da Silva, M.G.C. and Vieira, M.G.A. 2020. Removal of toxic metals from water using chitosan-based magnetic adsorbents. A review. *Environ. Chem. Lett.* 18. 1145-1168. Doi: <https://doi.org/10.1007/S10311-020-01003-Y>.
- [26] Kyriakopoulos, G.L., Tsimnadis, K., Sebos, I. and Charabi, Y., 2024. Investigating the effect of pore size distribution on the sorption types and the adsorption-deformation characteristics of porous continua: the case of adsorption on carbonaceous materials. *Crystals*. 14(8). 742. Doi: <https://doi.org/10.3390/cryst14080742>.
- [27] Sharifi, M.J., Nouralishahi, A. and Hallajisani, A. 2023. Fe<sub>3</sub>O<sub>4</sub>-chitosan nanocomposite as a magnetic biosorbent for removal of nickel and cobalt heavy metals from polluted water. *Int. J. Biol. Macromol.* 248. 125984. Doi: <https://doi.org/10.1016/j.ijbiomac.2023.125984>.